

Simulation of Inertia Friction Welding of Mild Steel and Aluminium 6061 using Finite Element Method on ABAQUS

Pushpandra Nimesh¹, Rajiv Chaudhary², R. C. Singh³, Ranganath M. S⁴

^{1,2,3,4} (Mechanical, Production & Industrial Engineering, Delhi Technological University, Delhi, India)

Email: pushpandranimesh3@gmail.com

Abstract : Friction welding is a welding technique based on green technology concept as it uses non-consumable tool to produce coalescence between the workpieces by utilizing heat generated due to friction and plastic deformation at the interface of workpieces affecting the formation of weld joint material in solid state. This technique can be used to producing joints on equipments utilizing traditional machine technologies for welding between varieties of similar and dissimilar metals & alloys and it also for producing weld joint between metal reinforced composites. Use of friction welded joints leads to a significant reduction in weight and cost savings. Friction welding process as a reusable tool for industrial and manufacturing sectors. Apart from industrial and manufacturing level applications, inertia friction welding process finds its application in field of Navy and Medicinal applications. Friction welding process seems to be a simple process but actually it is not so, Instead it is a very complex process as it includes conversion of mechanical energy into thermal energy in form of heat due to frictional rubbing between work-pieces. So prediction of properties of weld formed at interface is difficult. Numerical simulation offers a way to tackle such problems and also a way to increase repeatability of the friction welding process at manufacturing level and also it opens new ways to understand the process's mechanics more efficiently. This research works review an introduction toward the friction welding process, work that had been performed in corresponding field and research work needed to be done in the corresponding field on the basis of research gap in the corresponding field. This work consists of performing inertia friction welding process between mild steel and aluminum 6061 using lathe machine and then performing numerical simulation of the inertia friction welding process using finite element method on ANSYS and ABAQUS and then performing comparison of the data obtained both experimentally and numerically so as to increase the repeatability of the inertia friction welding process.

Keywords: Simulation, IFW- Inertia friction welding, Mild steel, Al 6061- Aluminum grade 6061, ABAQUS

INTRODUCTION

Friction welding process; being a welding process consist very less similarity with the conventional welding process instead it resembles to that of a forging operation. This method of welding process consists of providing continuous rubbing action between surfaces of a rotary work component and a stationary work piece whereby due to continuous frictional rubbing between work-pieces causing frictional heat to be generated at interface and then application of pressure causes plastic deformation at interface resulting formation of weld joint at interface. This welding technique termed as friction welding provides very simple and efficient way of joining work pieces together as compared to conventional fusion welding process. The method finds its application ranging from repairing cracks, joining members such as studs or bushes to another work pieces. Another aspect of the friction welding process comprises of causing a harder material probe to be entered into a softer material work component.

Friction welding process resembles much that to forge welding process which consists of producing weld joint with the application of pressure. According to basic fundamentals;

Heat is generated if two surfaces having frictional contact are allowed to be rubbed together. A certain large amount of heat can be generated with the help of frictional rubbing and certainly temperature can also be raised to such higher levels where the components having contact are just on verge of melting and thus allowed to be fused together causing welding of work- components.

Apart from friction welding process, Conventional welding process follows another technique. In conventional welding process, relative motion between work-pieces is restricted while welding tool is allowed to have motion. Quality of weld joint formed depends on motion of welding tool; too fast or too slow speed cause improper weld joint formation.

LITERATURE REVIEW

Over the last many years, simulation of inertia friction welding had been playing a major role in analysis of mechanics of inertia friction welding process and allowed to see the welding process from a different perspective.

Mumin Sahina et al performed modeling of Friction Welding process using Finite Element method. Mathematical expression between operating characteristics of friction

welding i.e. torque and heat energy produced because of friction welding was made under this paper. Obtained knowledge from numerical calculation study is valuable to develop the fundamental theory and engineering application research of friction welding.

Wenya Li et al performed Numerical Simulation of Friction Welding Processes Based on ABAQUS Environment. Temperature incurred during welding process was experimentally recorded and also numerical simulation is performed for estimation of temperature following comparison of two welded products.

Manthan Malde performed study under title Thermo-mechanical Modeling and Optimization of Friction Stir Welding involving generation of a thermo-mechanical model for studying the variation of temperatures encountered during real time friction stir welding process and then performing comparison of same with simulated data performed on ANSYS 11.0.

Sachin kumar et al published a research paper regarding the temperature modeling of friction welding process of aluminum and stainless steel-304. The welding process was carried out using a vertical milling machine. The studies include micro-structural study of weld joint and heat affected zone and creation of temperature profile for weld zone and HAZ. The results shows that during welding process , diffusion occurs at weld interface causing increase in concentration of Fe in aluminum part and a decrease in concentration of Fe in stainless steel part.

Sa.a.akbari mousavi et al conducted experimental and numerical analysis of the friction welding of the mild steel to mild steel and mild steel and 4340 steel combination. Research work was done to study the effect of welding parameters like friction, time, friction pressure, upset time, rotational speed etc. Studies include considering variations of temperatures, deformation, and strain rate during experiment and validating with simulated data. Numerical simulation was successful and every process parameters was in accordance with actual experimental data excepting the upset length which differs a lot on comparison with actual data.

Medhat el hadek performed a 3 dimensional axi-symmetric finite element analysis of inertial frictional welding of non-linear copper and Al 6061. Studies included welding time, rotational speed, thrust pressure i.e. the process parameters values as obtained from experiment after performing the Taguchi's optimization method. These values are given to FEM analysis as input on ansys. Transient thermal and dynamic structural analysis is performed on ansys. Studies mainly consist of comparison of deformation shape, upset shape in simulation with actual shape as in experiment. Deformation and upset shape as predicted from FEA was in accordance with the actual experimental results.

Yogender, Ranbir Singh published a research paper consisting of a case study on bimetallic welds. Studies included throughout review of a number of research papers. Studies reveal that a vast research is going in the fields of

friction welding process of similar and dissimilar materials. Research gap shows that upset length shape as predicted with proposed FEA model was not in accordance with the actual one. Also, no means to measure hardness value of the FEA model during numerical simulation.

N. Rajesh Hynes, P. shenbaga velu's research works consists of formulation of a thermo-mechanical model of the friction welding process using finite element method. Mathematical model was formed in accordance as the heat generated during friction welding process is due to friction and due to plastic deformation of the materials. Heat flux determination at the interface was modeled using unsteady 3-dimensional non-linear heat transfer equation. Heat generated during the plastic deformation was related with the Johnson-cook stress equation with the assumption that all mechanical energy is completed converted into heat energy at interface.

P. Ulysse presented a 3-D finite element model for studying effect of temperature and force on the tool in friction stir welding as a function of welding speed and rotational speed. Experimental data was collected by performing experiment on CINOVA 80 milling machine. Comparison of predicted data and experimental data shows that maximum temperature in both the cases decreases as welding speed increases and vice-versa if rotational speed of tool is increased. Forces acting on tip of FSW's tool increase as welding speed increases and decreases if rotational speed of tool is increased. Comparison of both data shows that temperature predicted by FEA was higher than experimental data and force prediction was found in accordance.

L.D Alvisé et al published a research paper regarding formulation of FEM for simulating inertia friction welding process between dissimilar materials. The studies include generation of thermo-mechanical model for predicting temperature of weld zone and HAZ. The agreement between temperature Prediction and experimental data reports a relative error of 6.6% while upset length comparison shows a relative error of 3.8%.

Wenyali Li et al conducted numerical simulation of friction welding process of mild steel combinations on ABAQUS using adaptive mesh control. The studies consist of using modified coulomb's law of friction at higher temperature as friction behavior convert into viscous-plastic friction. Temperature prediction by FE solver was in accordance with experimental data with a maximum error of 1.8%. FE model faced problem of element distortion while upsetting shape was found not in accordance with experimental data.

Hazman Seli et al published a research paper regarding mechanical evaluation and thermal modeling of inertia friction welding of mild steel and aluminum rods. Experiment was conducted on rotary drive friction welding machine. The studies also consist of construction of one dimensional FEM model using MATLAB and performing comparison with the experimental data. Comparison of both data shows temperature profile not to be in accordance due to problem in thermal modeling. Hardness and tensile strength

at weld zone was found lower than parent material due to incomplete welding.

Ji Shun de et al performed three Dimensional numerical analysis of material flow behavior and flash formation of steel in continuous drive friction welding using DEFORM-3D. Coulomb friction model was used to describe friction behavior at weld interface. Mesh generation near weld interface was done with considering fine element due to involvement of high temperature and coarse element in region of lower temperature. The studies shows that too small or too large flash formation and application of large axial pressure causes damage to service life of component being welded and stability of joint respectively.

In this research work, modeling of inertia friction welding process using finite element method including both thermal and mechanical aspects of the welding process had been performed.

EXPERIMENTATION

In this research work, the welding process was performed using lathe machine as rotation of one work component can be done easily. For fascillation of inertia friction welding process, a special fixture was prepared. The objective behind performing the experiment on lathe machine was to calculate optimum values of process parameters and then feeding these experimentally calculated values to the FEA software ABAQUS and performing the comparison between experimentally calculated and numerically simulated data.



Figure 1: Parent materials

During inertia friction welding process, torsional and translations vibrations produced are of very high magnitudes. In order to minimize these vibrations, special fixture was fabricated. This special fixture was a bottle type hydraulic jack of capacity two ton with a drill chuck attached to the piston of the jack using arc welding and at the base, a tapered rod having Morse taper was welded.



Figure 2: Special fixture

Design of experiment for this research work was carried on basis of Taguchi methodology. The Taguchi method basically is an optimization technique which involves reduction in error in a certain process with the help of its robust design of experiment's technique by making use of orthogonal arrays to arrange the process parameters and number of levels of each process's parameters in a tabular form. Use of these arrays results in significant reduction in number of experimental runs. Mild steel and aluminum 6061 rods were cut to required length and standard size specimen were prepared. In total eighteen samples were prepared by cutting them from parent materials rods based on Taguchi's orthogonal array, nine samples of mild steel and nine samples of aluminum 6061. Length of each cut samples was 60mm and diameter of samples were 25mm. Initially the aluminum work-piece was fixed on lathe chuck and mild steel work-piece was fixed in special fixture. Special fixture was attached to the tail stock. First step was to start the lathe machine by switching on. Mild steel and Al 6061 work-piece were attached to lathe's chuck and special fixture respectively. Lathe was given rotational motion by setting its rpm to pre-defined values of 1200, 780 and 460 rpm according to Taguchi's L9 array. Tail stock was given translational motion by rotating the wheel attached to it. Both mild steel and Al 6061 work-pieces were first allowed to have a gentle touch and then tail stock was advanced in direction of Al 6061 work-piece resulting in high frictional contact between mild steel and Al 6061 work-pieces. Due to frictional rubbing action between mild steel and Al 6061 work-pieces, large amount of heat generation takes place resulting in softening of material near contact region thus yield strength of both materials also decreased. Then a certain amount of pressure (forging pressure) application resulted in complete weld formation between mild steel and Al 6061 work-pieces. Good welding upsetting was observed at contact region.

Above procedure was repeated to produce nine weld jointed samples as per on the basis of Taguchi's optimization technique.



Figure 3: Experimentation



Figure 4: Welded work-pieces

Post welding processes includes calculation of process objectives or target values for fascillation of measuring performance characteristics of the inertia friction welding process so as welding process can be optimized. Process objectives or target values measured in this project study were measurement of hardness value of mild steel, Al 6061 and weld zone, measurement of impact energy of weld zone. Welded work-pieces were undergone by turning operation on lathe machine in order to obtain a uniform cross section throughout the length, So that fascillation of hardness and impact energy tests were done smoothly.

Table 1: Hardness values for Al 6061's heat affected zone

S. No.	Speed (RPM)	End conditions	Hardness (B-grade)
1	1200	With grinding	83
2	1200	No grinding	75.6
3	1200	With tapering	72.28
4	780	With grinding	79.03
5	780	No grinding	75.35
6	780	With tapering	80.65
7	460	With grinding	73.90
8	460	No grinding	78.38
9	460	With tapering	81.37

Table 2: Hardness values for Mild steel's heat affected zone

S. No.	Speed (RPM)	End conditions	Hardness (C-grade)
1	1200	With grinding	38.2
2	1200	No grinding	43.54
3	1200	With tapering	44.25
4	780	With grinding	53.88
5	780	No grinding	52.39
6	780	With tapering	49.13
7	460	With grinding	48.31
8	460	No grinding	60.04
9	460	With tapering	48.7

Table 3: Hardness value for Weld zone

S. No.	Speed (RPM)	End conditions	Hardness (C-grade)
1	1200	With grinding	32.55
2	1200	No grinding	50.2
3	1200	With tapering	40.5
4	780	With grinding	33.15
5	780	No grinding	43.05
6	780	With tapering	39.525
7	460	With grinding	41.77
8	460	No grinding	46.5
9	460	With tapering	41.67

Table 4: Impact energy data for welded samples

S. No.	Speed (RPM)	End conditions	Impact energy (Joules)
1	1200	With grinding	298
2	1200	No grinding	209
3	1200	With tapering	185
4	780	With grinding	210
5	780	No grinding	215
6	780	With tapering	278
7	460	With grinding	184
8	460	No grinding	248
9	460	With tapering	290

NUMERICAL SIMULATION WORK

Initially it was proposed to carry out numerical simulation of inertia friction welding process on Ansys 15.0 using finite element method but due to lack of better hardware connectivity and due to introduction of certain errors and to reduce computational solving time, later on numerical simulation was carried out on ABAQUS/CAE 6.10 software package. Inertia friction welding process, a solid-state welding process seems so simple but rather it is a very complex manufacturing process due to involvement of conversion of mechanical energy into thermal energy due to frictional rubbing action between the parent materials. To carry out simulation of inertia friction welding process, combined thermal and mechanical effects both needed to be considered and mathematical relation between them was needed. Mathematical equations defining relationship between thermal and mechanical aspect was used from research work done by Manthan Malde^[28]. Energy that was utilized in friction welding process was coming because of deformation due to plasticity (strain energy) and thermal energy flow due to frictional heating (heat energy). Both structural and thermal analysis (coupled structural-thermal) numerical simulation of inertia friction welding process was carried out. For modeling of thermal behavior of process's mechanics, Abaqus workbench software make use of general unsteady heat flow equation written in Cartesian coordinates

(given by eqn-1) is being used because of unsteady/transient thermal nature of welding process.

$$K [\partial^2 T / \partial x^2 + \partial^2 T / \partial y^2 + \partial^2 T / \partial z^2] + G = \rho c \partial T / \partial t \quad - (1)$$

Where k- thermal conductivity, T-temperature, G- heat generation rate, c-specific heat, ρ-density, t- time, and x, y, z are spatial coordinates.

Properties used in equation-1 are temperature dependent as using temperature independent properties can lead to improper modeling of thermal aspect of welding process. Table (5) and (6) shows temperature dependent material properties of mild steel and aluminum 6061 which were used in research work.

Table 5: Temp. Dependent properties of mild steel

S.NO.	Temperature (Celsius)	Thermal Conductivity (J/m-k)	Heat Capacity (J/kg-k)	Density (kg/m ³)	Thermal Expansion (10 ⁻⁶ K ⁻¹)	Young's modulus (GPa)	Poisson ratio
1.	0	34.5	470	7890	1.6	220	0.28
2.	98	34.5	485	7860	1.65	200	0.3
3.	201	33.8	520	7870	1.7	194	0.32
4.	316	31	560	7840	1.8	186	0.28
5.	428	28.5	620	7690	1.85	179	0.29
6.	571	26.8	700	7440	1.9	172	0.28
7.	650	25.8	760	7430	1.95	165	0.25

Table 6: Temperature dependent properties of aluminum 6061

S.NO.	Temperature (Celsius)	Thermal Conductivity (J/m-k)	Heat Capacity (J/kg-k)	Density (kg/m ³)	Thermal Expansion (10 ⁻⁶ K ⁻¹)	Young's modulus (GPa)	Poisson ratio
1.	0	264	917	2703	22.4	69.7	0.33
2.	98	253	978	2685	24.61	66.2	0.33
3.	201	223	1028	2657	26.6	59.2	0.33
4.	316	207	1078	2630	27.6	47.78	0.33
5.	428	192	1133	2602	29.6	31.72	0.33
6.	571	177	1230	2574	34.2	20.91	0.33
7.	650	162	1235	2538	36.3	15.38	0.33

Heat generated due to plastic deformation is simulated by using command QRATE (Quinney plastic coefficient) in Abaqus command prompt which defines the proportion of thermal heat generation as a result of strain energy release due to plastic deformation occurring in the material. Generally QRATE is taken with a value of 0.9. Plastic deformation work is given by eqn -3

$$W_p = \int \sigma \cdot d\epsilon \quad - (3)$$

W_p multiplied by QRATE defines the G_p as used in equation-2

Heat generated due to frictional heating is given by multiplication of frictional force at the contact point and the surface sliding /rubbing velocity as given by eqn - 4.

$$W_f = F_f * V_f \quad - (4)$$

Abaqus workbench module readily follows coulomb classical law of friction as per definition of contact interaction

occurring in problem. This research study assumes Coulomb classical law of friction. As per definition of coulomb classical friction law, friction force (F_f) is directly proportional to normal force (F_n) by coefficient of friction (μ) as given by $F_f = \mu * F_n$ - (5)

As per definition of frictional work, is given by

$$W_f = \mu * F_n * V_f \quad - (6)$$

W_f multiplied by frictional heat weightage factor (Π) gives us the heat generation rate due to irreversible plastic deformation of parent materials given by eqn- 7.

$$G_p = \mu * F_n * V_f * \Pi \quad - (7)$$

Construction of geometry was done using ABAQUS design modeler software package. Geometry consists of two concentric solid cylinder of diameter 15mm and length 60mm as per sample description by ASME. Then defining the desired element type was next step to perform. Choosing

suitable element type in a simulation problem is of very much need. Element type SOLID226 was used for defining solid elements. CONTA 173 was used for defining contact element region and TARGE170 WAS used for defining target element region of contact interaction region. SOLID226, CONTA173, TARGE170; solid and contact element type was used because of their coupled structural and thermal degree of freedom as inertia friction welding process is a coupled structural-thermal complex process which requires use of spatial and temperature degree of freedom both. Due to involvement of frictional and deformable contact definition proper modeling of contact surface was much needed. Modified Lagrange algorithm was used to define the contact stiffness algorithm. Effects of initial penetration at contact region and separating gap between contact surfaces was eliminated using certain user subroutines commands. Boundary conditions used in the research work was mild steel work-piece was given translational motion ($U1=U2=UR1=UR2=UR3=0, U3\neq 0$), aluminum 6061 work-piece was allowed to have only rotational degree of freedom along z-axis ($U1=U2=U3=UR1=UR2=0, UR3\neq 0$) convection heat loss to surrounding environment by both work-pieces, radiation heat loss to surrounding environment by both the work-pieces. Meshing plays a crucial part in performing numerical simulation of a process. Meshing generally implies discretization of whole working model into a small number of elements known as finite elements. Finite elements resembles to that of like grains in a material. In this research work, hexagonal type brick mesh elements were used to assign meshing to both fixed and rotary work pieces along with use of Lagrangian type mesh algorithm for assigning mesh control to both work-pieces.

Table 7: Pressure load variation with according to time

S.NO.	Time (Sec)	Pressure (MPa)
1-	0	0
2-	0.2	5
3-	0.4	10
4-	0.6	15
5-	0.8	20
6-	1.2	25
7-	1.4	30
8-	1.6	30
9-	1.8	30
10-	2.0	30
11-	2.2	30
12-	2.4	30
13-	2.5	30
14-	2.7	30
15-	2.9	30
16-	3.2	30
17-	3.4	30
18-	3.5	30

Table 8: Angular velocity variation with according to time

S.NO.	Time (Sec)	Angular Velocity (RPM)
1-	0	0
2-	0.2	10
3-	0.4	30
4-	0.6	40
5-	0.8	50
6-	1.2	70
7-	1.4	80
8-	1.6	90
9-	1.8	100
10-	2.0	105
11-	2.2	105
12-	2.4	105
13-	2.5	105
14-	2.7	0
15-	2.9	0
16-	3.2	0
17-	3.4	0

As during inertia friction welding process, plastic flow of both the parent materials occurs. So defining plastic behavior of both parent materials is of much need. Johnson-cook plasticity model was used for defining plastic flow characteristics of mild steel and aluminum 6061. Johnson-cook model was used as it provides strain, temperature, strain rate dependent flow stress properties.

The Johnson–Cook flow stress model is purely empirical in nature and it defines the relationship between flow stresses, melting temperature, and strain rate. Johnson-cook model is given by:

$$\sigma_Y(\epsilon_p, \dot{\epsilon}_p, T) = [A+B(\epsilon_p)^n] [1+C \ln(\dot{\epsilon}_p^*)] [1-(T^*)^m]$$

Where ϵ_p is the plastic strain, $\dot{\epsilon}_p$ is the plastic strain-rate, and A,B,C,n,m are material constant.

Table 9: Johnson-cook model parameters for mild steel

	A(MPa)	B(MPa)	N	C
Mild steel	217	233.7	0.6428	0.0756

Table 10: Johnson-cook model parameters for aluminum 6061

	A(MPa)	B(MPa)	N	C	M
Aluminum 6061	289.6	203.4	.35	0.011	1.34

In this project work, as due to meshing size and as well as due to non-linearity associated with the friction welding process, computational time was initially was very large ; so large deflection was activated by using command- NLGEOM,ON to facilitate plastic behavior of parent materials.

Step size controls were totally replaced with new steps controls. Simulation was done for a total of 3.5 seconds with auto time stepping set to on; along with initial step size of 0.001 seconds, minimum step size of 0.0008 seconds, and maximum step size of 0.002 seconds.

RESULTS AND DISCUSSION

After completion of simulation of inertia friction welding process of mild steel and Al 6061, various results were obtained regarding its deformation, temperature distribution, stress distribution, strain induced, strain energy, heat generated due to plastic deformation and frictional contact at weld zone and heat affected zone.

Results obtained after completion of simulation of inertia friction welding process of mild steel and Al 6061 were compiled together in form of graphs, figures showing distribution of these results on parent materials, weld zone and heat affected zone and later on comparison between simulated and experimentally calculated data was performed in order to check feasibility of simulation of Inertia friction welding process between mild steel and Al 6061.

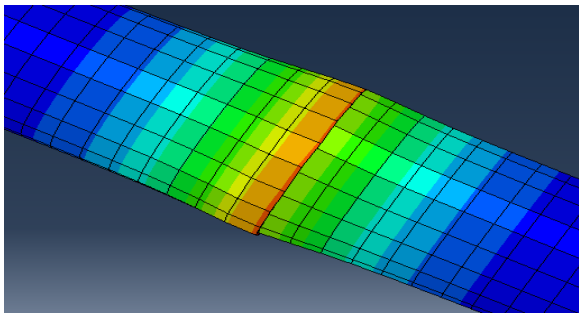


Figure 5: Deformed contact after completion of simulation process

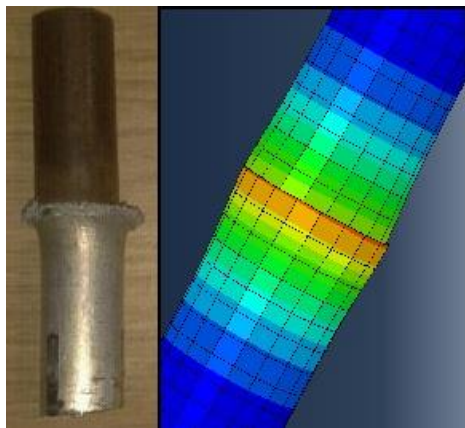


Figure 6: Comparison of upsetting length

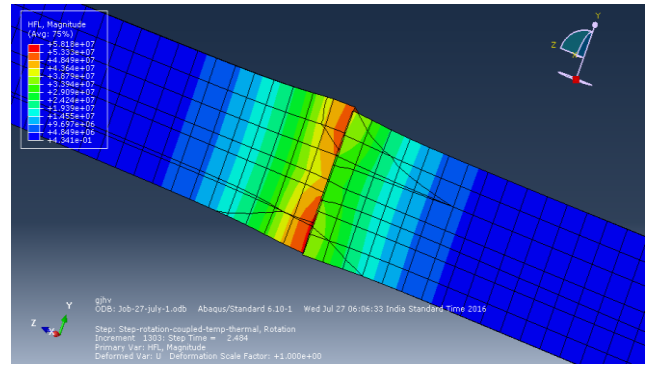


Figure 7: Heat flux distribution near weld zone and HAZ with free cut

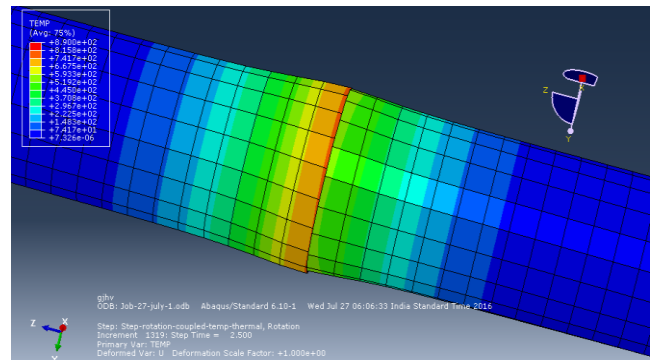


Figure 8: Temperature distribution near weld zone and HAZ

The graph given below represents the temperature distribution in finite elements at weld zone

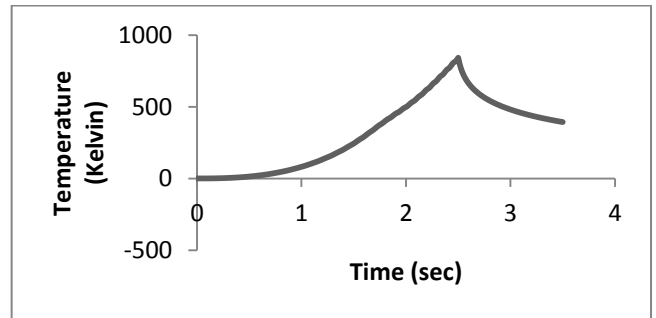


Figure 9: Temperature distribution at weld zone with respect to time

The graph given below represents the temperature distribution in finite elements in heat affected zone of mild steel. For defining heat affected zones, 8mm line from the weld zone i.e. toward mild steel were taken as reference for defining heat affected zone.

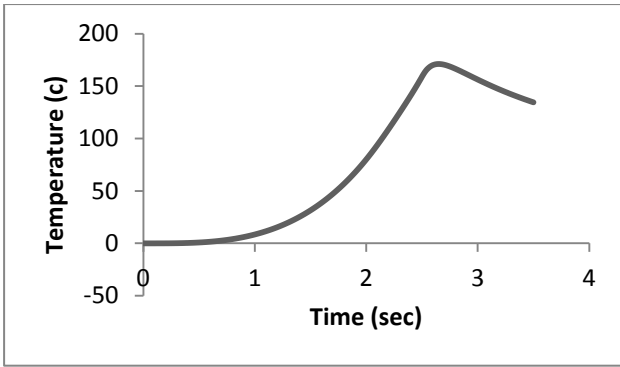


Figure 9: Temperature distribution at HAZ of Mild steel with respect to time

The graph given below represents the temperature distribution in finite elements of heat affected zone of Al 6061. For defining heat affected zones, 2mm line from the weld zone i.e. toward Al 6061 was taken as reference for defining heat affected zone.

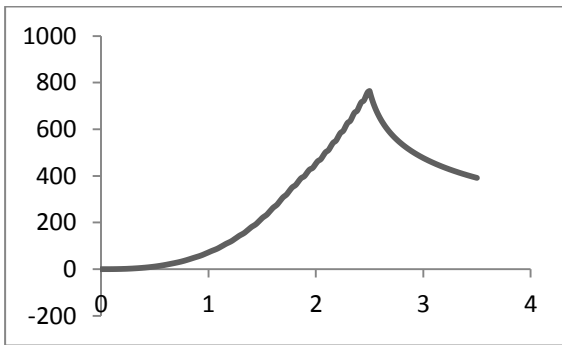


Figure 10: Temperature distribution at HAZ of Al 6061 with respect to time

The graphs given below represent the Heat flux distribution in finite elements of weld zone with respect to time. X- Axis represents time in seconds. Y- Axis represents heat flux in Watt per unit area.

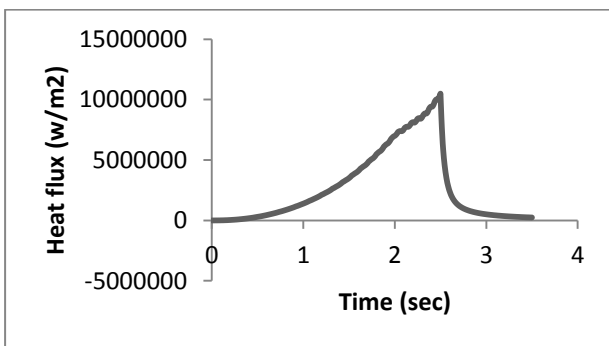


Figure 11: Heat flux distribution at weld zone with respect to time

The graphs given below represent the distribution of Von-Mises stress generated in finite elements of weld zone with respect to time. X- Axis represents time in seconds. Y- Axis represents Von-Mises stress in Pascal.

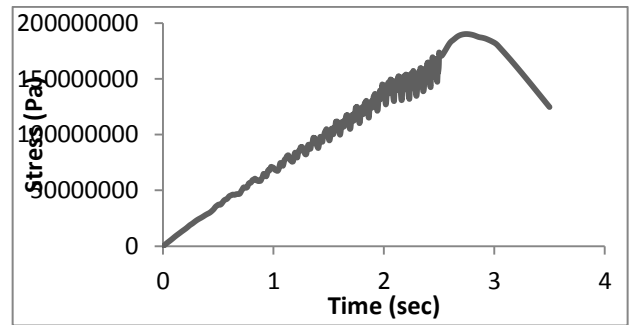


Figure 12: Von-Mises stress distribution at weld zone with respect to time

The graphs given below represent the distribution of Tresca stress generated in finite elements of weld zone with respect to time. X- Axis represents time in seconds. Y- Axis represents Tresca stress in Pascal.

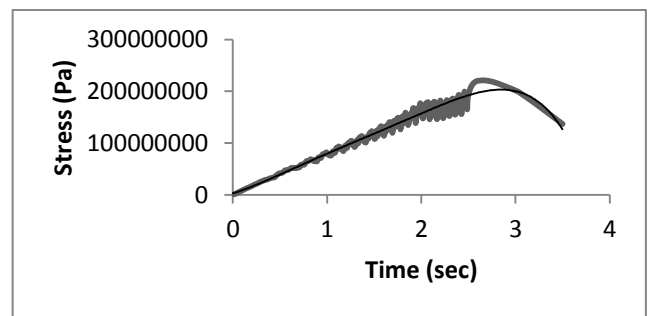


Figure 13: Tresca stress distribution at weld zone with respect to time

The graphs given below represent the distribution of Maximum principle stress generated in finite elements of weld zone with respect to time. X- Axis represents time in seconds. Y- Axis represents Maximum principle stress in Pascal.

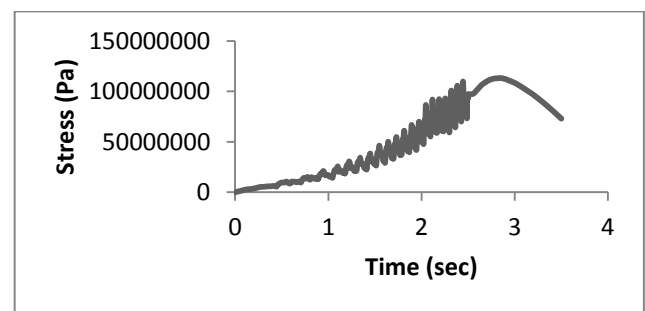


Figure 14: Max. Principle stress distribution at weld zone with respect to time

The graphs given below represent the distribution of elastic limit strain generated in finite elements of weld zone with respect to time. X- Axis represents time in seconds. Y- Axis represents elastic strain in meter/meter.

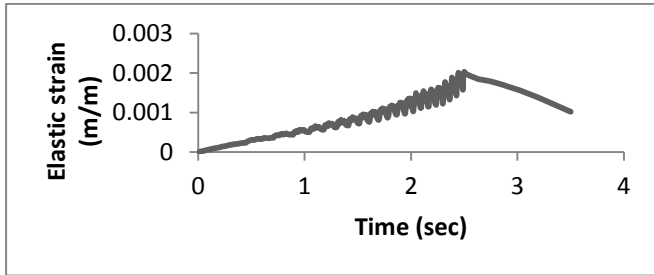


Figure 15: Elastic strain distribution at weld zone with respect to time

The graphs given below represent the distribution of logarithmic strain generated in finite elements of weld zone with respect to time. X- Axis represents time in seconds. Y- Axis represents logarithmic strain in meter/meter.

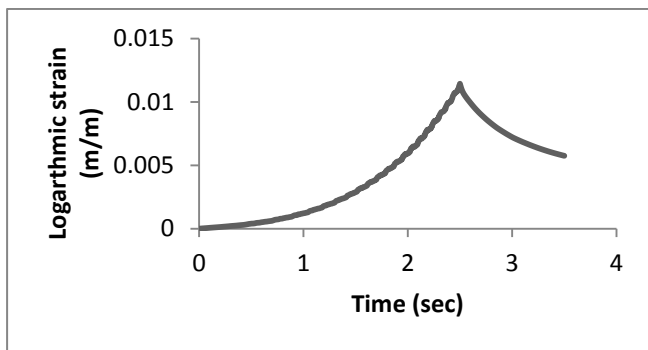


Figure 16: Logarithmic strain distribution at weld zone with respect to time

The graphs given below represent the distribution of plastic strain data generated in finite elements of weld zone with respect to time. X- Axis represents time in seconds. Y- Axis represents plastic strain in meter/meter.

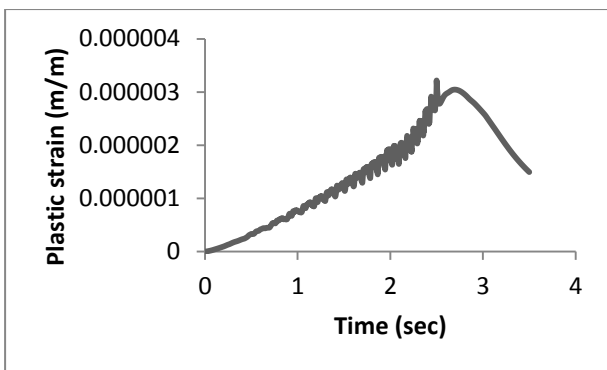


Figure 17: Plastic strain distribution at weld zone with respect to time

The graphs given below represent the distribution of strain energy density data absorbed in finite elements of weld zone with respect to time. X- Axis represents time in seconds. Y- Axis represents plastic strain in meter/meter.

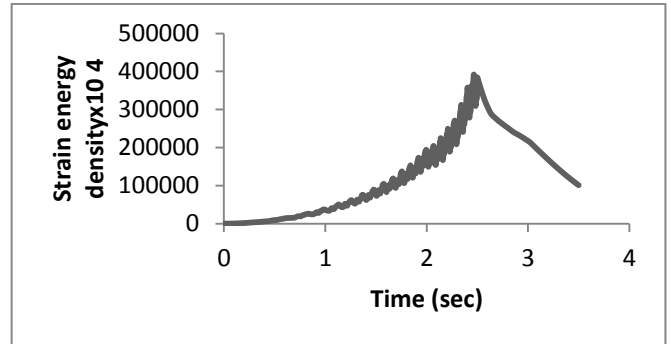


Figure 18: Strain energy distribution at weld zone with respect to time

The graphs given below represent the distribution of frictional energy generated in finite elements of whole model due to frictional rubbing between work-pieces with respect to time. X- Axis represents time in seconds. Y- Axis represents Frictional energy in joule.

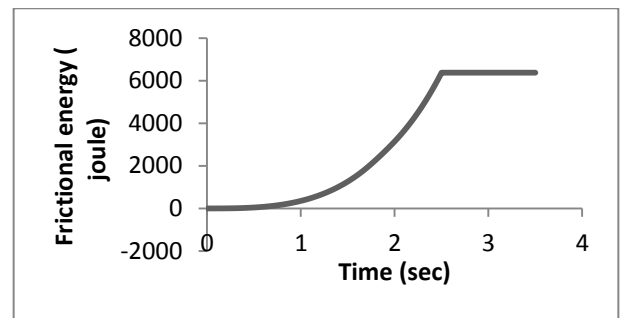


Figure 19: Frictional energy distribution of work-piece with respect to time

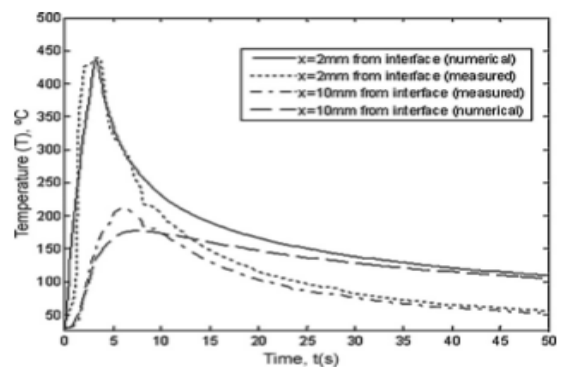


Figure 20: Experimentally calculated temperature data for Al 6061 work-piece at a distance of 2mm from weld interface [25]

From the above figure, it is clear that peak temperature rise during inertia friction welding process are of order 400-430 °c for heat affected zone of Al 6061.

CONCLUSIONS

Corresponding to temperature distribution at weld zone interface for total weld time, it was observed that highest peak temperatures achieved while performing simulation of inertia friction welding process was in the range of 800-900 Kelvin i.e. 527-627 Celsius which was close to melting point temperature of Al 6061 which caused Al 6061 finite element model to cause yielding and undergoes plastic deformation to form upsetting.

Comparison of data obtained experimentally and data obtained numerically for HAZ of Al 6061 at a distance of 2mm from welding interface shows a good agreement.

Peak temperature obtained from numerical simulation at Al 6061 HAZ was in order of 480- 490 Celsius while experimental data shows a peak temperature of 450 at Al 6061 HAZ. These results show a good agreement with themselves with a relative error of 8.35% in measurement of temperature from numerical simulation as compared with experimentally calculated temperature data.

Comparison of upsetting length observed during experimentation and that obtained from numerical simulation shows a good agreement related to the shape of upsetting extruded out of the weld zone interface.

REFERENCES

- [1] Alexandre Mathieu, Rajashekar Shabadi, Alexis Deschamps, Michel Suery, Simone Mattei, Dominique Grevey, Eugen Cicala, Dissimilar Material Joining Using Laser Aluminum To Steel Using Zinc-Based Filler Wire, Elsevier, 39 (2007) 652–661.
- [2] S.H. Hashemi, D. Mohammadyani, Characterization of Weld Joint Hardness, Impact Energy and Microstructure in Api X65 Steel, Elsevier, 98 (2012) 8-15.
- [3] Ahmet Hascalik , Nuri Orhan, Effect Of Particle Size On The Friction Welding Of Al2o3 Reinforced 6160 Al Alloy Composite And Sae 1020 Steel, Elsevier, 28 (2007) 313–317.
- [4] N. O Zdemir A, F. Sarsilmaz A, A. Hasc, Alik B, Effect Of Rotational Speed On The Interface Properties Of Friction-Welded Aisi 304L To 4340 Steel, Elsevier 28 (2007) 301–307.
- [5] Mumin Sahin, H. Erol Akata, Kaan Ozel, An Experimental Study On Joining Of Severe Plastic Deformed Aluminum Materials With Friction Welding Method, , Elsevier, 29 (2008) 265–274.
- [6] M.N. Ahmad Fauzi, M.B. Uday, H. Zuhailawati, A.B. Ismail, Microstructure And Mechanical Properties Of Alumina-6061 Aluminum Alloy Joined By Friction Welding, Elsevier, 31 (2010) 670–676.
- [7] H. Khalid Rafi, G.D. Janaki Ram, G. Phanikumar, K. Prasad Rao, Microstructure And Tensile Properties Of Friction Welded Aluminum Alloy Aa7075-T6, Elsevier, 31 (2010) 2375–2380.
- [8] A.K. Lakshminarayanan, V.Balasubramanian, an Assessment of Microstructure, Hardness, Tensile and Impact Strength of Friction Stir Welded Ferritic Stainless Steel Joints, Elsevier, 31 (2010) 4592–4600.
- [9] Hazman selia, Ahmad Izani Md. Ismailb, Endri Rachmanc, Zainal Arifin Ahmadd, Mechanical Evaluation And Thermal Modeling Of Friction Welding Of Mild Steel And Aluminum, , Elsevier, 210 (2010) 1209–1216.
- [10] Shubhavardhan R.N & Surendran S, Friction Welding To Join Stainless Steel And Aluminum Materials, International Journal Of Metallurgical & Materials Science And Engineering (IJMSE) Issn 2278-2516 Vol.2, Issue 3 (2012) 53-73.
- [11] Sandeep Kumar1, Rajesh Kumar And Yogesh Kumar Singla, To Study The Mechanical Behavior Of Friction Welding Of Aluminum Alloy And Mild Steel, International Journal Of Metallurgical & Materials Science And Engineering, Issn (2278 – 0149), Vol.1, No. 3 (2012).
- [12] Mumin Sahin, Mahmut Kucuk, Modelling Of Friction Welding, Trakya University Faculty of Eng. And Arch. Dept. Mech. Eng. 22180, Edirne-Turkey Dept. Mech. Eng. 22180, Edirne-Turkey (2012).
- [13] I. Alfaro G, Racineux A. Poitou, E.Cueto, F. Chinesta, Numerical Simulation Of Friction Stir Welding By Natural finite element Methods Aragón Institute Of Engineering Research (2009).
- [14] Dranasyaghi and Professor Adib Becker State Of The Art Review - Weld Simulation using Finite Element Methods University Of Nottingham, UK.
- [15] Sachin Kumar, Deepak Bhardwaj, Jagdeep Sangwan , A Research Paper on Temperature Modelling of Friction Welding of Aluminum and Stainless Steel-304, (2014).
- [16] S.a.a.Akbari Mousavi, A. Rahbar Kelishami, Experimental and numerical Analysis of the Friction Welding Process for the 4340 Steel and Mild Steel Combinations, (2008).
- [17] Medhat a. El-Hadek, Numerical Simulation of the Inertia Friction Welding Process of Dissimilar Materials, (2014).
- [18] Yogender, Ranbir Singh, A brief Research Review of Bimetallic Welds, (2012).
- [19] N Rajesh Jesudoss Hynes and P Shenbaga Velu, Thermo Mechanical Modelling of Friction Welding using Finite Element Method, (2015).
- [20] Rajesh Kumar, Lalit Kumar, Discussion on Tensile Test of Friction Welded Specimen of Aluminum Alloy 6063 and Stainless Steel 304, (2015).
- [21] Finite Element Analysis of Friction Welding Process for Dissimilar Materials, page no.171-191.
- [22] P. Ulysse, Three-dimensional modeling of the friction stir-welding process, (2002).
- [23] L.D Alvise, E.Massoni, S.J. Walloe, Finite element modeling of the inertia friction welding process between dissimilar materials, (2002).
- [24] Wenya Li, Shanxiang Shi, Feifan Wang et al, Numerical simulation of inertia friction welding process based on ABAQUS environment, (2012).
- [25] Hazman Seli, Ahmad Izani Md. Ismail et al, Mechanical evaluation and thermal modeling of friction welding of mild steel and aluminum, (2010).
- [26] Ji Shun De, LIU Jian Guang et al, 3-D Numerical analysis of material behavior and flash formation of steel in continuous drive friction welding, (2012).

- [27] Kleiber, M & Sluzalec Finite Element Analysis of Heat Flow in Friction Welding, Engineering transactions, vol. 32, 107-113 (1984).
- [28] Manthan Malde, Thermo-mechanical Modeling and Optimization of Friction Stir Welding involving generation of a thermo-mechanical model on ANSYS 11.0.
- [29] Ranganath M Singari, Vipin, Sanchay Gupta, Prediction of Surface Roughness in CNC Turning of Aluminum 6061 Using Taguchi Method and ANOVA for the Effect of Tool Geometry, International journal of advanced production and industrial engineering, Vol 1(1), 22-27
- [30] Ranganath. M. S., Vipin, R.S. Mishra, Prateek, Nikhil Optimization of Surface Roughness in CNC Turning of Aluminum 6061 Using Taguchi Techniques, International Journal of Modern Engineering research (IJMER), volume 5, Issue 5, May 2015,42-50
- [31] Ranganath M. S., Vipin, Nand Kumar, R Srivastava, "Surface Finish Monitoring in CNC Turning Using RSM and Taguchi Techniques". International Journal of Emerging Technology and Advanced Engineering Website Volume 4, Issue 9, 2014, 171-179.
- [32] Ranganath M. S, Applications of TAGUCHI Techniques in Turning (AKN Learning, Delhi: Delhi, 2015).
- [33] www.wikipedia.com.
- [34] www.sciencedirect.com.
- [35] www.ansys.com
- [36] www.abaqus.com
- [37] www.google.com